Recyclable Clay-Supported Heteropolyacid Catalysts for Complete Glycolysis and Aminolysis of Post-Consumer PET Beverage Bottles

Gopal Jeya
Pachaiyappa's College
Elumalai Ganesan
University of Tsukuba Faculty of Pure and Applied Sciences: Tsukuba Daigaku Daigakuin Suri Busshitsu Kagaku Kenkyuka
Aimi Asilah Haji Tajuddin
University of Tsukuba Graduate School of Pure and Applied Sciences: Tsukuba Daigaku Daigakuin Suri Busshitsu Kagaku Kenkyuka
Yoshikazu Ito
University of Tsukuba Faculty of Pure and Applied Sciences: Tsukuba Daigaku Daigakuin Suri Busshitsu Kagaku Kenkyuka
Ravikumar Dhanalakshmi
Pachaiyappa's College
Vajiravelu Sivamurugan (sivaatnus@gmail.com)
Pachaiyappa's College https://orcid.org/0000-0002-9295-2118

Research Article

Keywords: Aminolysis, Depolymerisation, Glycolysis, Heteropolyacids, PET wastes, Chemical recycling, Circular economy

Posted Date: October 25th, 2021

DOI: https://doi.org/10.21203/rs.3.rs-1002767/v1

Abstract

In this investigation, the use of phosphotungstic acid (PWA) and phosphomolybdic acid (PMA) as well as Zn^{2+} containing kaolin and bentonite explored for chemical recycling of post-consumer poly(ethyleneterephathalate) (PET) wastes have been explored. The clay supported catalysts containing 5wt% of the metals and heteropolyacids (HPAs) are synthesized using wet impregnation method. The effect of metal ions and HPAs loading on the surface area, pore volume, elemental composition and crystalline nature of the kaolin and bentonite has been evaluated by nitrogen adsorption and desorption studies, SEM-EDX mapping, powder XRD, FTIR and XPS analysis. The total surface area of BET increased with a loading of 5 wt% of Zn^{2+}, PWA and PMA on kaolin and bentonite, while the pore volume and pore diameter remain unchanged. SEM and EDAX mapping images showed that the heteropolyacids crystals are well dispersed on the surface and occupied interlayer spaces of the clay support. SEM-EDX showed that bentonite showed a better loading of PWA and PMA compared with kaolin. PET waste water bottles collected from the local market used for the chemical recycling process. The aminolysis reaction using Zn^{2+} and PWA loaded on bentonite showed complete depolymerisation of PET wastes to produce 87-98% of BHETA. The glycolysis reaction using the above catalysts showed complete depolymerisation at 180-210 °C and yielded 78-90% of BHET. When comparing the clay, bentonite performed well in terms of heteropolyacid loading and afforded a higher yield of BHET and BHETA due to higher loading of Zn and HPA as supported by SEM-EDX and XPS. Reusability of the catalysts were also examined for glycolysis.

Introduction

The chemical recycling process for post-consumer polyesters such as PET and PLA could contribute to the development of circular economy, in which the valorisation of polyesters through chemical depolymerization into value added monomers (Thomas et al. 2020; Payne and Jones, 2021). PET waste recycling methods are classified into four main techniques for implementing plastics recycling: primary (closed loop), secondary (mechanical), tertiary (chemical), and energy recovery (combustion) (Chen et al., 2021; Singh et al., 2016). Preferably, the PET recycling can be performed by two main approaches viz., mechanical recycling (Sinha et al., 2010) and chemical recycling (Wang et al., 2015; Lamberti et al., 2020) in order to recover either pure polymer or terephthalic acid derivatives respectively. The chemical recycling process, especially the depolymerization of PET waste, is considered using heterogeneous catalysts as an economical and eco - friendly method of recycling plastic waste since depolymerized products could be reused to produce PET (Liguori et al., 2021) or polyurethane foams for automotive applications (Bedell et al., 2018).

Chemical recycling, namely, glycolytic transesterification using ethylene glycol (EG) (or) diethylene glycol (DEG) or any other glycol of PET chains yields bis(2-hydroxyethyl) terephthalate, it is a substrate for PET synthesis in monomer or oligomers (Maurya et al., 2020). Most PET glycolysis depolymerization is widely studied in the presence of EG catalyzed by Zn^{2+} salts or any other acidic catalyst (Al-Sabagh et al., 2015; Singh et al., 2017), ionic liquids and deep eutectic solvents (Xin et al., 2021) or by using enzyme catalysts

(Zimmermann, 2020) and microorganisms such as *Microbacterium oleivorans* and *Thermobifida fusca cutinase* (Yan et al., 2021). Likewise, the aminolysis reaction could be used for the efficient depolymerization of PET polymer into terephthalamide derivatives (Gupta, 2019). The depolymerisation of PET polymer using various amines etc, allylamine, morpholine, hydrazine, and polyamines have been investigated (Langer et al., 2020).

The heterogeneous catalyst for chemical transformation (Nagasundaram et al., 2020) of PET waste could be quickly and thoroughly depolymerized into its monomer bis(2-hydroxyl ethyl) terephthalate (BHET). In an eco-friendly approach, ash obtained from orange peel (Lalhmangaihzuala et al., 2021) and bamboo leaf fly ash catalyst (Laldinpuii et al., 2021) were used as a catalyst for PET depolymerization that yields 79 and 83% of the recrystallized product, respectively. These catalysts are non-toxic, renewable, accessible and inexpensive catalysts for glycolysis of post-consumer polyethylene terephthalate waste. In parallel, inorganic metal oxide-based catalysts have contributed to the glycolytic and aminolytic depolymerization of PET wastes. For example, the glycolysis of PET waste has been accomplished through Mg-Al-O@Fe_3O_4 nanoparticles (Guo et al., 2021). The aminolytic depolymerisation of PET wastes achieved using hydrazine monohydrate, as a novel homogeneous catalyst and advantageous with respective to cost effectiveness and more reactive towards degradation of PET polymer. The reaction recorded a significantly higher yield of up to 84% within 2 hours at 65 °C and the final product is terephthalic dihydrazide, a useful intermediate (George et al., 2016) and ethylene diamine as an aminolyte agent (Hoang et al., 2013; More et al., 2017). Chemical recycling of PET waste is accomplished by ionic liquids, metal salts, enzymes, and hydrotalcites as catalysts (Khoonkari et al., 2015).

Kaolin clays provide solid support due to their inherent acidity, excellent thermal stability, and generally attractive structural features, such as easily controlled structure morphology (Attique et al. 2018). Therefore, acidified with kaolin with a large specific surface area is widely used as a wonderful catalytic carrier for many organic transformations (Nagendrappa, 2011; Maya et al., 2016; Hajizadeh et al., 2020;) and furfural converted into cyclopentenones (Bonacci et al., 2019). Heteropolyacid like phosphomolybdic acid supported bentonite used for the biowaste into biofuel as a Bronsted acid catalyst (de Oliveira et al., 2019). Heteropoly acids are concentrated solid acids that have ubiquitous applications in various fields (Chen et al., 2018; Kundu et al., 2013), and value-added products from lignin (Guan et al., 2020). The mixture of bentonite is montmorillonite (85%) and other contaminants Etc, illite, quartz, chlorite, and calcite. The montmorillonite structure consists of three layers, an octahedral-shaped alumina layer in the middle surrounded by two layers of tetrahedral silica (SiO_4) form. The octahedral and tetrahedral layers contain monovalent and bivalent cations such as Na^+, Ca^{2+} and Mg^{2+}. This arrangement leads to the creation of interior space and a charging interlayer (Siregar et al., 2018). Recently, more attention has been focused on heteropoly acids (HPAs) because of their many advantages, which are also known as eco-friendly and economically viable alternatives to conventional acid catalysts because of their Bronsted acidity, high proton mobility, relatively excellent and chemical stability (Chen et al., 2019; Shuangjun et al., 2020).

In our previous study, the effect of aluminium, zinc and iron containing kaolin and bentonite catalysts have been evaluated for the depolymerization of PET polymer using glycolysis was reported (Jeya et al., 2017; Jeya et al., 2019). Among them, Zn^{2+} loaded bentonite showed better results than kaolin analogue as well as other metals. From our observation as well as from reported literature, the acidity of the catalyst playing a key role in triggering the glycolysis reaction. Based on our investigation, presently, we have investigated depolymerisation of the post-consumer PET soft drink bottles collected from the local market using glycolysis and aminolysis process catalysed by heteropolyacids impregnated kaolin and bentonite catalysts and the same compared with Al^{3+} and Zn^{2+} loaded clay analogues. To prepare economically viable catalysts, commercially available clay supports were purchased and the ion was exchanged with Al^{3+}, Zn^{2+} and phosphomolybdic and phosphotungstic acids and characterized using BET, XRD, FT-IR, XPS and SEM and the structures of depolymerized products, N1,N4 -bis(2-hydroxyethyl)terephthalamide (BHETA) and bis(2-hydroxyethyl)terephthalate (BHET) is confirmed by ^{1}H NMR, ^{13}C NMR and mass spectra. Hence, in the present investigation, the glycolysis and aminolysis reaction using heterogenous catalysts, we could expect that reaction proceed in clean and pure product could be obtained. Therefore, the ^{1}H NMR, ^{13}C NMR and mass spectra were run for the crude product isolated from the reaction mixture. In view of the above claims, the process could be economical and environmentally sustainable.

Experimental

Materials

Clay supports and other reagents such as Kaolin, bentonite, aluminum nitrate, zinc nitrate, phosphotungstic acid (PWA), and phosphomolybdic acid (PMA) were purchased from SRL, India and Loba, India and used without further purification. All the glasswares and quick-fits we employed in the experimental work were made up of corning/borosil glass. These glasswares were washed thoroughly and dried in a hot air oven before use.

Wet impregnation of Heteropolyacids and metal ions into clay catalysts

The metal ions or HPAs impregnated at 5 wt% loadings into kaolin and bentonite catalysts with respect to clay weight were prepared. In this method, for loading percentage of Zn^{2+}, Al^{3+} ions and HPA for varied while the amount of clay was kept constant. It was produced by stirring 5wt% of Zn^{2+} using $Zn(NO_3)_2$, Al^{3+} using $Al(NO_3)_3$, as a metal-ion source dissolved in 50 mL of distilled water containing 10g of clay and the mixture stirred well at 100 °C for 12 hrs. The impregnated catalysts were isolated by filtration followed by washing with 2 x 50 ml of distilled water and then the clay catalysts dried in the oven at 90 °C for 6 hours. The dried clay samples were kept in a desiccator during the study of this investigation.

Characterization of clay catalysts

The synthesized catalysts characterized by using XRD to determine crystalline nature of the catalysts, while the surface area and pore diameter of the catalysts were obtained from the nitrogen absorption and desorption analysis. The XRD analyzed performed on BRUKER D2 PHASER (XE-T Edition) using powder X-ray diffraction at 2θ angle between 10 and 80 and operating at 9.0 kW (CuKa radiation = 1.5406Å). Nitrogen adsorption and desorption measurements were made on a volumetric gas adsorption apparatus (BELSORB MAX, Japan, Version: 1.3.12). The average pore diameter and average pore volumes were calculated using the adsorption branch of the N_2 isotherms based on the Barrett-Joyner-Halenda (BJH) model. The specific surface area of the catalysts was calculated using the BET equation. The Fourier transformed infrared spectra in the transmittance mode are reported in the range 400 to 4000 cm^{-1} at room temperature using the KBr disc technique spectrometer (IRTracer-100, Shimadzu). The FT-IR spectra used to identify the presence of functional groups of the catalysts with respect to characteristic vibrational peaks. The morphology and elemental compositions were determined via SEM-EDX of the original clay and ion-exchanged clay materials received by the scanning electron microscope (SEM, JCM – 7000 measurement data). The spin-orbit coupling using XPS (AXIS Ultra DLD, Shimadzu) measured binding energy.

Catalytic Activity

The catalytic activity of 5wt% of Zn^{2+}, Al^{3+}, PWA and PMA loaded kaolin and Bentonite has been studied toward glycolysis and aminolysis of PET waste using ethylene glycol as glycolyte reagent and ethanolamine as aminolyte reagent under normal atmospheric conditions except reaction temperature (Scheme 1).

General procedure for Glycolysis of PET wastes using ethylene glycol

In the typical glycolysis reaction of PET wastes, 1 g of crushed PET chips was added to a 100 ml two neck flask containing 20 ml of preheated ethylene glycol medium (Preheated ethylene glycol at 130-150 ° C for quick dissolution of PET chips). The mixtures were stirred well using a magnetic stirrer and heated to 180 – 210 ° C. Temperature of the reaction system was maintained using a temperature controller. After reaching the optimal temperature, 50 mg of catalyst (5 wt% with respect to PET weight) was added. After 2 hr time interval, 0.5 mL of reaction mixture was diluted by acetone and the reaction progress monitored using pre-coated aluminium TLC plates (E-Merck, UK, Silicagel G60 F254 indicator) containing 356 nm UV indicator. The spots were eluted using n-hexane and ethyl acetate (70:30) solvent mixture the spots were identified using a UV detector using a 356 nm light source. When the reaction is completed, the mixture was added to 100 ml of distilled water and then filtered through Whatman paper to remove the catalyst. The filtrate was kept at 5 ˚C for 24 h and the needle-shaped crystal formed, then filtered on whatmann filter paper to collect the depolymerized sample and dried at room temperature. Finally, from the weight of the precipitate the yield of the reaction is calculated.

General procedure for Aminolysis of PET wastes using Ethanolamine

Similar to the glycolysis reaction, the aminolysis reaction is carried out using 1g of crushed waste PET polymer chips was taken in 100 ml two-necked flask and to that 10 mL of ethanolamine was added (preheating of ethanolamine not necessary for the aminolysis reaction). The reaction is heated to 150 – 160 ° C and maintained using a controller. After completion of the reaction, the mixture was diluted with water, and the catalyst was removed by simple filtration. The reaction filtrate kept under 5 ˚C for 24 hrs and aminolysed product obtained as light yellowish crystals. From the weight of the product, the yield is calculated with respect to the PET weight.

Characterization of depolymerized products

The depolymerized products BHET and BHETA were identified using ^{1}H and ^{13}C NMR spectra of the products obtained from glycolysis and aminolysis reactions respectively were recorded using $CDCl_3$ as a solvent and TMS as an internal standard (Bruker Avance III operating at 500 MHz). In addition, the mass spectrum also recorded using (Shimadzu, LCMS-2020, ionization method: EI) and recorded the FT-IR spectrum using the KBr pellet technique (Shimadzu, IRTracer 100).

Results And Discussion

Synthesis Of Catalysts

The commercially available kaolin and bentonite clay were purchased from Loba Chem Pvt. Ltd, India and used without further purification for the impregnation with $Zn^{2+}$and Al^{3+} nitrate salt and heteropolyacids were used. The wet impregnation method was successfully employed for the metal-ions loading process (Sen Gupta and Bhattacharya, 2008). The 5% weight load on the metal ions, however, a weight loss of 1-2 % weight was observed when drying at 80 ° C due to loss of moisture content in the clay sample. The synthesized catalysts were characterized by nitrogen adsorption and desorption, FTIR, powder X-ray diffraction (PXRD), SEM with EDX mapping, and XPS studies.

Bet Surface Area Analysis

Pore volume, pore size distribution, and BET surface area are essential characteristics of porous material to act as a catalyst or catalyst support. The catalytic activity of clay material could be correlated with modification of surface area and pore volume before and after loading of metal ions (Al^{3+} and Zn^{2+}) and heteropolyacids (PWA and PMA). The impact on porosity modification obtained from nitrogen adsorption-desorption studies. BET adsorption-desorption studies are extensions of Langmuir theory applied for multilayer adsorption on a homogeneous surface. The study is very helpful for finding gas-solid adsorption systems. The BET study is enabling the determination of the specific surface area of the catalysts. In addition to BET, the BJH model has been used to determine the average pore volume and pore diameter of porous materials. Since nitrogen gas is a non-reactive on acid or base surfaces, nitrogen adsorption-desorption isotherm used as a tool to build the BET and BJH model for the determination of

surface area and pore details. In Figure 1a and 1b, the results of the nitrogen adsorption and desorption isotherms of kaolin and bentonite impregnated with Zn^{2+}, PWA, PMA and Al^{3+} compared to pure kaolin and bentonite, respectively. The average pore diameter calculated from the BJH model and the average pore distribution are given in supplementary information **Figure S1.** The calculated BET surface area and average pore diameter and pore volume calculated using the BJH model are summarized in Table 1.

The typical adsorption and desorption of N_2 gas with respect to relative pressure (P/Po) have been recorded. It is interesting to note that, Kaolin supported catalysts showed Type II adsorption isotherm **(**Figure 1a**)** and bentonite supported catalysts showed Type IV adsorption pattern with clear Hysteresis loop **(**Figure 1b**).** The type II and IV adsorption pattern indicates the presence of both macro- and mesoporous nature of clay materials (Kuila and Prasad, 2013). The formation of hysteresis loop indicates capillary condensation of gas molecules in the mesopores (Wang et al., 2020). In Figure 1b, it is very interesting to note that pore widening is occurring while impregnation of 5wt% of PMA, PWA and Zn^{2+} on the bentonite support. On the other hand, the impregnation of metals and heteropoly acids did not show a significant effect on the porous nature of the kaolin support. The uptake of N_2 occurring at relative pressure of 0.48-0.52 indicates micropore filling. Average pore size distribution in supported kaolin and bentonite catalysts showed in supplementary information **Figure S1.** The average pore distribution showed the presence of the micro- and mesoporous nature of the clay materials. Impregnation with metals and heteropoly acids has a clear impact on surface area and pore size (Table 1).

Table 1
BET Surface area, pore volume and pore diameter of Kaolin and Bentonite catalysts

Catalyst	BET surface area (m^2/g)	Pore volume (cm^3/g)	BJH average pore diameter (nm)
Kaolin	6.602	0.0483	2.43
Al-Kaolin(5 wt%)	16.309	0.0522	1.66
Zn-Kaolin(5 wt%)	12.504	0.0512	2.76
PWA-Kaolin (5 wt%)	11.557	0.0435	2.14
PMA-Kaolin (5 wt%)	19.449	0.0605	1.22
Pure Bentonite	14.533	0.0317	1.66
Al-Bentonite (5 wt%)	19.803	0.0316	1.66
Zn-Bentonite (5 wt%)	23.684	0.0820	1.88
PWA-Bentonite (5 wt%)	18.303	0.0605	1.22
PMA-Bentonite (5 wt%)	23.949	0.0832	1.22

In our previous studies on bentonite and kaolin clay using BET and BJH revealed that bentonite exhibits a surface area of 19.1 m^2/g with a pore volume of 0.071 cm^3/g and a pore diameter of 15.79 nm. Similarly, the kaolin clay showed a surface area of 5.1 m^2/g with an average pore volume of 0.0200 cm^3/g and a pore diameter of 17.36 nm. In the present study, the pure kaolin (Figure 1a) showed BET surface area 6.602 m^2/g with pore volume 0.0483 cm^3/g and pore diameter 2.43 nm. However, it is interesting to note that ion exchange with Al^{3+}, Zn^{2+}, PWA and PMA showed notable changes in surface area and porosity, as discussed earlier (Table 1). The impregnation of 5 wt% loading of metal ions or heteropolyacids is increased in surface area from 12.504, 16.309 and 19.449 m^2/g, and pore volume increased from 0.0483, 0.0522 and 0.0605 cm^3/g for Zn^{2+}, Al^{3+} and PMA respectively. In contrast pore diameter is decreased from 2.43 to 2.14, 1.22 and 1.66 nm for ion exchanged kaolin catalysts. Similarly, the pure bentonite clay (Figure 1b) showed BET surface area 14.533 m^2/g with pore volume 0.0317 cm^3/g and pore diameter 1.66 nm. Like the effect of loading on kaolin, the specific area, pore volume, and pore diameter of the bentonite catalysts increased (Table 1). For example, especially for PWA, Zn^{2+} and PMA an increase in surface area from 14.533 to 23.949 m^2/g, pore volume from 0.0317 to 0.0832 cm^3/g, respectively. As compared to pure kaolin and bentonite, 5wt% PMA kaolin and bentonite showed a tremendous increase in the surface area and pore volume and marginal variation was observed in surface area and porosity for Zn^{2+}, PWA and Al^{3+}- exchanged clay catalysts.

Xrd Pattern Of Kaolin And Bentonite Catalysts

The powder XRD patterns of pure kaolin and bentonite, as well as ion exchanged analogues, have been recorded at 2 theta angles in the range of 10 and 80 °. The pure kaolin, bentonite and ion-exchanged catalysts are presented in Figure 1c and 1d. XRD analysis can be used to determine mineralogical composition of the clay catalysts. To find the effect of impregnation on the crystalline nature, the diffraction pattern of a catalyst supported by 5% metal ions and HPA was compared with pure kaolin and bentonite (Wang et al., 2020). Bentonite is consists of 7-39, 0.4 to 21, 30-75, and 5-20% kaolinite, montmorillonite, quartz, and cristobalite respectively. However, the main crystalline phases of bentonite are montmorillonite and quartz. Bentonite forms lattice structures consisting of a single plate located between alumina and silica plates. Owing to the layer system, montmorillonite may be expanded, and contract upon impregnation with metal ions. On the other hand, the crystalline nature could be completely collapsed due to exceeding the loading capacity limit of impregnation. The loading of metal ions and heteropolyacids could be expected to occupy the inter-layer space of montmorillonite that can be reflected by the size of its intermediate space (d001 and d020) of montmorillonite (Naswir et al., 2013). The diffraction pattern of supported bentonite clay Zn^{2+}, PWA, PMA and Al^{3+} catalysts was confirming a sharp peak at 2θ value of 26.80° that is attributed to the reflections of (001) plane of bentonite clay **(**Figure 1c**)**. The peaks were found at 19.90° and 24.96° at all samples, revealing the presence of a narrow amount of quartz with bentonite catalysts. The decreased in the (d001 and d020) interval indicates an increased in interlayer space owing to the impregnation of metal ions respectively (Jeya et al., 2019; Bouraie et al., 2017). Moreover, XRD pattern of pure and catalyst supported with bentonite catalysts showed similar crystalline pattern representing that the impregnation is not affected the bentonite framework.

The crystalline nature of kaolin clay and Zn^{2+}, PWA, PMA, and Al^{3+} catalyst containing kaolinite was confirmed by the presence of a sharp peak at 2θ value of 29.10° at which they are responsible for the reflections of (001) plane of clay **(**Figure 1d**)**. The peak at 62.50 ° at 2θ the reflection by a (060) plane indicates well-crystallized kaolin. The diffraction peak at 19.25 ° and 25.10 ° was also observed in all samples, revealing the presence of a small amount of quartz along with kaolin catalysts (Shukla et al., 2008; Jeya et al., 2017). Since the diffraction patterns of 5wt% of Zn^{2+}, PWA, PMA and Al^{3+} loaded clay is almost similar to that of pure kaolin, it is assumed that the impregnation process does not make any significant impact on the crystalline nature of the clays. Similar XRD patterns also suggest that loading up to 5.0wt% does not affect the crystalline nature of the catalyst. In addition, the retaining of porous nature of supported clay catalysts have been confirmed by N_2 adsorption and desorption studies.

Ft-ir Analysis Of Supported Clay Catalysts

The FTIR spectra of raw kaolin and wet impregnation samples of 5wt% Zn, PWA, PMA and Al-kaolin samples in the wave number range of 4000-400 cm^{-1} are shown in Figure 1e (Whole FT-IR spectra given in the supplementary information, **Figure S2**). The infrared spectra of the kaolin absorption band at 820 cm^{-1} and 860 cm^{-1} are attributed to Si-O-Al vibrations, and the band at 960 cm^{-1} is assigned to Al-OH

bend vibration. The broad peak at 1060 cm^{-1} corresponds to Si-O –Si in plane vibration and at 1130 cm^{-1} allocated to asymmetric Si-O-Si stretching vibration (Olaremu, 2015). The band appears at 3700 cm^{-1}, associated with hydroxyl group consistent with the kaolin layer. However, the band at 1100 cm^{-1} and 800 cm^{-1} to 760 cm^{-1} did not gain prominence, as they were intertwined with a strong band of silica in favor of kaolin (Aher et al., 2021a).

The FT-IR spectrum of bentonite and supported bentonite catalysts containing Al^{3+}, Zn^{2+}, PWA and PMA are shown in the supplementary information, Figure 1f (Whole FT-IR spectra given in the supplementary information, **Figure S3**). The IR spectra of pure and supported bentonite recorded in the region of 4000 – 400 cm^{-1}, and the bands are comparable and similar to the bentonite structure. The bands at 1058 cm^{-1} and 900 cm^{-1} correspond to the Si-O stretching vibration and OH bending mode of vibration, respectively (Al-Sabagh et al., 2015). The bands appearing at 460-532 cm^{-1} correspond to Mg-O stretching vibration (Morgan et al., 2004). A broad band appears at 3424 cm^{-1}, it is corresponding to OH asymmetric and symmetric stretching vibrations of M-OH, and a band at 1638 cm^{-1}, which is similar to bending vibrations of d-OH. The band appears at 3700 cm^{-1}, corresponding to the hydroxyl moiety of the bentonite layer (Russell et al., 1994). The infrared spectrum of PWA/Bentonite exhibits identical bands at 2800 and 2872 cm^{-1}, which correspond to the C-H stretching of the alkyl chain. The band appears at 1360 cm-1 and corresponds to carbonyl moiety symmetric stretching vibrations. The existence of characteristic groups of Zn^{2+}, Al^{3+}, PWA, and PMA impregnated in kaolin and bentonite is very difficult to ascertain from FT-IR due to overlapping of peaks.

Sem-edx Mapping Analysis

SEM analysis combined with EDX elemental mapping used to find elemental composition and the presence of impregnated catalytic sites in clay framework. Figure 2a-c and 3a-c summarises the impregnated kaolin and bentonite catalysts respectively analyzed by EDX analysis to find out the percentage of elemental composition (whole SEM-EDX images, elemental mapping given in supplementary information, **Figure S4** and **S5)**. Similarly, the estimated composition of supported kaolin and bentonite catalysts summarised in **Table S1** (supplementary information) and Table 2 respectively. Figure 2a and Table S1 show the mass and atomic percentage of Zn^{2+} in the Zn2 + impregnated kaolin catalyst and the weight percent composition of Zn^{2+} with respect to Al^{3+} and Si^{4+} is found to be 0.16±0.03%. The EDAX spectrum showed (Figure 2a) showed presence of Zn^{2+} and values of elemental mapping signifies that the impregnation of Zn^{2+} is less. On other hand, according to Figure 2b indicates EDAX spectrum of PWA loaded kaolin catalyst. The wet impregnation of PWA in kaolin is found to be very significant and the% mass of W^{6+} is found to be 3.43±0.10% when compared to Al^{3+} and Si^{4+} and theoretically we have synthesized 5wt% of PWA containing kaolin with respect to the weight of W^{6+} in PWA. The mass% of W^{6+} is found to be close with theoretical % of W^{6+}. On the contrary, the composition

of Mo^{6+} from PMA loaded with kaolin showed 0.18±0.02% of Mo^{6+}, which is found to be much lower compared to the theoretical value (Figure 2c).

Apart from the elemental composition, SEM images clearly showing the surface morphology of the supported catalysts is similar to pure kaolin. There is no change in the morphology of the catalyst proves that phosphotungstic acid and phosphomolybdic acid species are scattered well into the hexagonal holes (Aher et al., 2021a). Further, it is confirmed by X-ray diffraction analysis and BET surface area analysis.

Figure 3a is SEM-EDX analysis of Zn^{2+} loaded bentonite support. EDX analysis revealed that the mass and elemental composition of Zn^{2+} is 3.73±0.16 and 1.18±0.05% respectively (Table 2). It is interesting to note that the amount of Zn^{2+} loading is found to be higher when compared with kaolin supported analogue. Although similar experimental conditions have been followed, the bentonite is showing excellent loading capacity, especially in supported clay catalysis. We have clearly seen that with respect to catalytic activity towards depolymerization of post-consumer PET wastes using bentonite impregnated with Zn^{2+} and Al^{3+} performed excellently while comparing kaolin-supported analogues (Jeya et al. 2017; Jeya et al. 2020). The SEM-EDX spectrum of PWA loaded bentonite is shown in Figure 3b and Table 2, respectively. The SEM-EDX analysis confirmed the presence of W^{6+} and the composition of PWA-bentonite showed 14.74±0.12 wt% of W^{6+} in bentonite clay. It strongly indicates the successful impregnation of PWA in bentonite catalysts (Aher et al., 2021b). EDX analysis also revealed the presence of other elements present in bentonite clay, namely, Na^{+} in 2.01±0.03, Mg^{2+} in 1.13±0.02, Al^{3+} in 8.56±0.05, Si^{4+} in 19.12±0.07, Ca^{2+} in 1.60±0.03 and $Fe^{2+/3+}$ in 4.90±0.08% (Siredar et al., 2018). Figure 3c is the EDX spectrum of PMA loaded bentonite. The percentage of mass of Mo^{6+} was found to be 1.06±0.03%, while compared to the kaolin support, bentonite was found to be the best catalytic support with a higher metal ion loading capacity (Aher et al., 2021b). Comprehensively, the mass and atomic % values signify that amount of PWA and PMA loading on bentonite support is higher compared to PWA and PMA supported kaolin catalysts. FT-IR results in clear agreement with SEM-EDX studies, this indicates continued layer broadening of bentonite. In addition, the BET surface area analysis showed increasing surface area of bentonite and kaolin support upon PMA and PWA loading. The higher loading capacity of bentonite resulted in higher catalytic activity, which eventually afforded excellent yield of a pure glycolyzed and aminolyzed single product, BHET and BHETA.

EDX analysis of pure bentonite showed that the presence of O, Na, Mg, Al, Si, Ti, Fe and similar components have been present in 5wt% of impregnated bentonite catalysts with Zn^{2+}, PWA and PMA and SEM images along with elemental mapping and EADX spectrum given in Figure 8a-c respectively (Munir et al., 2019). The mass and elemental composition of impregnated bentonite catalysts are summarized in the supplementary information Table 2.

Table 2
SEM- EDX mapping Mass percentage and atomic percentage of bentonite catalysts

Elements	5wt% Zn-Bentonite		5wt% PWA-Bentonite		5wt% PMA-Bentonite	
	Mass%	Atomic %	Mass%	Atomic %	Mass%	Atomic %
O	51.69±0.19	67.08±0.25	47.33±0.15	68.57±0.21	54.38±0.15	69.05±0.19
Na	2.38±0.04	2.15±0.04	2.01±0.03	2.03±0.03	3.06±0.04	2.70±0.03
Mg	2.52±0.04	2.15±0.03	1.13±0.02	1.07±0.02	1.45±0.02	1.21±0.02
Al	10.62±0.07	8.18±0.05	8.56±0.05	7.36±0.04	9.70±0.05	7.30±0.04
Si	22.00±0.10	16.26±0.08	19.12±0.07	15.78±0.06	22.61±0.08	16.35±0.06
K	2.14±0.04	1.14±0.02	0.48±0.01	0.28±0.01	0.45±0.01	0.24±0.01
Fe	4.45±0.10	1.65±0.04	4.90±0.08	2.03±0.03	5.39±0.08	1.96±0.03
M*	**3.73±0.16 (Zn)**	**1.18±0.05 (Zn)**	**14.74±0.12 (W)**	**1.86±0.02 (W)**	**1.06±0.03 (Mo)**	**0.22±0.01 (Mo)**

*M – Metal loadings from Zn, W from PWA, and Mo from PMA

Analysis Of The Morphology Of Supported Catalysts

The SEM images (supplementary information, **Figure S6**) and Figure 2d-f show the surface morphologies of the kaolin before and after wet impregnation of Zn^{2+}, PWA and PMA respectively. SEM images revealed that no notable modifications in the morphology on pure kaolin (Figure S6) and ion- exchanged metal ions **(**Figures 2d, 2e and 2f**)** have been observed. However, at a closer look at higher magnification (7000X, 2 µM) the layered structure of clay can be clearly seen in Fig. 2d-f. The clear appearance of layered structure could be due to broadening of inter layer distance because of impregnation of PMA and PWA, which is higher molecular size (Winiarsk et al., 2018).

Similarly, the SEM images of pure bentonite and Al^{3+} impregnated bentonite (supplementary information, Figure S7) and Zn^{2+}, PWA, PMA, and Al^{3+} loaded bentonite are clearly shown in Figure 3d **– f**, respectively. The SEM images showed the morphology of bentonite clearly consist of stacked layered structure (Winiarsk et al., 2018; Aher et al., 2021b). Due to the layered structure, the SEM imaging showed the effects of impregnation on clay supports. In pure bentonite clay (**Fig. S7a**), the layered nature of clay is not clearly visible even at higher magnification (3000X, 5 µM). Whereas Figure 3d and S7b are Zn^{2+} and Al^{3+} incorporated bentonite showed rough surface and deformed layered structure. However, the XRD studies confirmed that the crystalline nature of bentonite is retained even after metal ion loading. More interestingly, the PWA loaded bentonite showed small crystallite PWA crystals deposited on the surface **(**Figure 3e**)**. The resulting surface morphology of the PWA/bentonite catalyst is completely different from

that of pure bentonite. The SEM images clearly showed that PMA is homogeneously dispersed on the surface of the bentonite (Figure 3f).

Xps- Analysis And Elemental Composition

The chemical composition of Zn^{2+}, Al^{3+} and HPA loaded kaolin and bentonite was recorded by X-ray photoelectron spectroscopy (XPS). The XPS spectra of Kaolin and bentonite supported Zn^{2+}, PWA and PWA catalysts are shown in Figure 2g-i and 3g-i, and binding energy (eV), metal to Al^{3+} ratio and atomic composition is summarised in **Table S2** and **S3** of supplementary information, respectively. Figures 2g and 3g are the XPS spectra of Zn^{2+} loaded kaolin and bentonite, respectively. Zn^{2+} loaded kaolin as well as bentonite support showed two peaks at 1022 and 1045 eV are the binding energies of $Zn2p_{3/2}$ and $Zn2p_{1/2}$, which is related to the spin-orbit splitting of about approximately 22 eV. The metal-to-Al^{3+} ratio of bentonite showed a higher content of Zn^{2+} loading compared to catalysts supported by kaolin. Due to this higher loading capacity, the bentonite supported catalysts showed higher catalytic activity towards depolymerisation of PET wastes in glycolysis and aminolysis reaction. All XPS spectra showed a symmetric peak approximately at 533 eV that was O_2^- connected to Si and attributed to SiO_2 based materials and summarized in the Supplementary Material, **Figure S8 to S19**.

Figure S13b and S19b showed binding energy peaks of Al^{3+} in Zn^{2+} loaded kaolin and bentonite. XPS analysis revealed the presence of binding energies of 2pA and 2pB for Al^{3+} approximately at 74.72 and 75.75 eV in kaolin and bentonite-supported catalysts. Figures 2h and 3h are the peaks of W^{6+} binding energy in phosphotungstic acid (PWA). The presence of W^{6+} in PWA supported on kaolin and bentonite is confirmed by the binding energy peaks at 36.06 and 38.19 eV attributed to spin-orbit coupling $4f_{7/2}$ and $4f_{5/2}$ states. The mineral composition of W^{6+} to Al^{3+} is found to be 0.07 (7%) and 0.11 (11%) with respect to Al^{3+} for kaolin and bentonite loaded with PWA, respectively. Thus, the presence of a higher loading of PWA in bentonite was attributed to the higher catalytic activity. In the case of, kaolin and bentonite loaded with phosphomolybdic acid (PMA) showed Mo^{6+} spin orbit coupling binding energy peaks approximately at 233 and 236 eV, which is attributed to transition states $4d_{5/2}$ and $4d_{3/2}$ (Figure 2i and 3i). Similarly, bentonite showed higher phosphomolybdic acid (PMA) loading is observed from the elemental composition of Mo^{6+}, which is estimated to be 0.04 (4%) and 0.13 (13%) for PMA loaded kaolin and bentonite respectively.

Figure S13e and **S13f** is spin-orbit coupling peaks of Al^{3+} in Al^{3+} loaded kaolin and bentonite respectively. The binding energy peaks at 75.50 and 74.50 eV, which corresponds to Al 2pB and Al 2pA. Similarly, pure kaolin and bentonite showed binding energies of Al^{3+} at 75.60 and 74.60 eV, which corresponds to the spin-orbit coupling states of Al 2pB and Al 2pA.

Depolymerisation of PET waste using glycolysis and aminolysis

Glycolysis and aminolysis are the common depolymerisation reaction applied for PET wastes. The presence of ester linkage in the PET polymer chain enables the hydrolysis using acids or bases to give terephthalic acid. However, the ester linkage could be cleaved using methanol to give dimethylterephthalate (DMT) as the final product through the transesterification reaction. However, the methanolysis process needs a high-pressure reactor to overcome the pressure built by a low-boiling methanol solvent. By using a similar transesterification methodology, ethylene glycol or ethanolamine has been used to depolymerise PET waste to generate bis(2-hydroxyethylene)terephthalate (BHET) or bis (2-hydroxyethylene) terephthalamide (BHETA), respectively. However, a Lewis or Bronsted acid catalyst required to activate the ester carbonyl group and trigger the transesterification reaction and higher reaction temperature is required for the dissolution of PET chips in ethylene glycol for the complete depolymerisation of PET.

Thus, in the present investigation, an economical catalyst support, clay material has been opted to prepare Lewis and Bronsted acid supported catalyst. Ethylene glycol has been used as a glycolyting agent as well as solvent. The depolymerisation reaction has been carried out in the presence of 10wt% of the clay catalyst.

In both cases, Figures 4a and 4b, the glycolysis and aminolysis of PET waste using kaolin and bentonite clay loaded with Zn^{2+}, PWA and PMA, respectively. The use of ethylene glycol (EG) and ethanol amine (EA) as a common depolymerizing agent for glycolysis and aminolysis process. The glycolytic depolymerisation lead to monomer, bis(hydroxyethyl)terephthalate (BHET) and aminolytic depolymerisation lead to monomer, bis(hydroxyethyl)terephthalaimide (BHETA). In both depolymerisation reactions, we have observed complete depolymerisation of PET wastes. The final product isolated from the reaction mixture is highly pure is confirmed by ^{1}H and ^{13}C NMR, in which the peaks correspond to PET oligomers were absent. The reaction time is 6-7 hrs for glycolysis, whereas the aminolysis required only 4-5 hrs for the complete depolymerisation. The reaction was monitored by TLC using an ethylacetate to hexane ratio at 20:80. After completion of the reaction, the reaction mixture was diluted with hot water (100 mL) and filtered to the catalyst. After filtration, the reaction mixture was heated to 60 ˚C for 15 min and kept at 5 ˚C for 24 h for the glycolysis reaction and after heating the reaction mixture kept room temperature for 24 h for the aminolysis reaction mixture. In the case of glycolysis, we identified issues associated with the isolation of the final product from water because the product is water soluble. However, the final product is obtained completely by extraction with chloroform and the final yield is calculated. In the case of aminolysis, the final product BHETA is obtained as pale yellowish needle crystals from the reaction mixture at room temperature itself. We have tried with many diamines for aminolysis, ethanol amine is worked better at low temperature and afforded excellent yield of BHETA. The crystals of BHETA filtered, dried and yield of the reaction calculated. Both ^{1}H and ^{13}C NMR, and mass spectral analysis showed BHETA is a single pure product.

Figures 4a and 4b are the result of the glycolysis and aminolysis reaction. In the case of glycolytic depolymerization reactions, Zn^{2+} and PWA loaded bentonite-supported clay catalysts gave 92 and 93% of BHET, respectively, when compared with kaolin-supported analogues. On other hand, the aminolytic

depolymerisation reaction revealed that Zn^{2+} and PWA loaded bentonite afforded 94 and 96% of BHETA respectively in comparison with kaolin supported analogues. Similarly, the glycolysis reaction was performed with ethylene glycol as the transesterification catalyst. In both reactions, the bentonite clay support found to be the better catalytic support as it is supported by BET surface area analysis, SEM-EDX, and XPS analysis.

Catalysts Recycling Studies

The PWA and Zn^{2+} loaded kaolin and bentonite catalysts were subjected to recycling studies using glycolysis as a model reaction. At the end of each reaction cycle, the spent catalysts were filtered following washed with water and dried in the oven before the next reaction cycle. The yield of the depolymerized product obtained from the subsequent reaction cycle was compared **(**Figure 4c**)**. The study revealed that the catalyst can be reusable up to six cycles with marginal loss in yield. Among the catalysts, PWA and Zn^{2+} loaded bentonite catalysts showed better results. Higher catalytic activity of bentonite catalyst could be correlated with higher surface area of bentonite, which eventually can take more PWA and Zn^{2+} as supported by BET, SEM -EDX and XPS studies. The slower leaching of PWA from the surface and interlayer spaces is reflected in the yield of the BHET formed.

SPECTRAL ANALYSIS OF DEPOLYMERISED PRODUCTS

All depolymerized products would have been characterized by ^{1}H, ^{13}C NMR, and mass spectroscopy to confirm the structure.

^{1} H NMR spectrum

The four aromatic hydrogens present in BHET have appeared **(Supplementary information, Figure S20)** as singlets 8.08 ppm confirm the formation of the glycolyzed product, the BHET monomer. The ^{1}HNMR run for the crude product showed singlet aromatic protons that confirmed the complete depolymerization of PET wastes (Sarkar et al., 2014). In the case of BHET, the two hydrogens attach to carbon next to the ester carbonyl oxygen appeared as a triplet at 4.47 ppm. Another two hydrogens attached to carbon next to OH has appeared as triplet at 3.97 ppm. The former appeared downfield due to the presence of electron-withdrawing carbonyl oxygen attached. The OH proton appears as a broad singlet at 3.70 ppm due to the exchangeable nature of its kind. The deuterated $CDCl_3$ solvent appeared as singlet 7.26 ppm (Jeya et al., 2017; Jeya et al., 2020). Similarly, the ^{1}H NMR of the crude depolymerized product obtained from the aminolysis of PET using 2-amino ethanol is given in the Supplementary information **(Figure S21).** The main aminolyzed product N^{1},N^{4}-bis(2-hydroxyethyl)terephthalamide (BHETA) is a symmetrical molecule. Hence, the four aromatic hydrogens present in the central aromatic ring of BHETA were appeared as singlet 8.07 ppm confirming the formation of aminolysed product BHETA and complete depolymerisation of PET wastes. The two N-H protons of the amide linkage attached to the methylene group are observed as a triplet at 8.74 ppm and the -OH protons of the alcoholic group are observed at

2.64-2.65 ppm as a triplet (Ghosal et al., 2019). In the case of BHETA, the two hydrogens attach to carbon next to amide carbonyl oxygen, and -NH appeared as a triplet at 3.48-3.51 ppm. Another two hydrogens attached to carbon next to OH has appeared as triplet at 3.65-3.68 ppm. Therefore, presence of –N-H and–O-H protons confirms the 2-amino ethanol attached to terephthalaoyl group to form the BHETA.

^{13} C NMR spectrum

^{13}C NMR spectrum of BHET is shown in supplementary information **(Figure S22)**. The ester carbonyl carbon of BHET appeared at 166.16 ppm is showing single ester carbonyl present the structure and no other carbonyl carbons were recorded, which confirmed the presence of BHET as a single product. Since BHET is a symmetrical molecule, here are two aromatic carbons that appeared at 133.80 and 129.70 ppm. The peak at 133.80 ppm corresponds to C-1 and C-4 attached to ester carbonyl, and another peak at 129.70 corresponds to C-2, C-3, C-5 and C-6 attached with hydrogen appeared as singlet with high intensity. The -CH_2- carbons of the aliphatic chain attached to the ester carbonyl oxygen appeared at 67.0 ppm for BHET. The variation in –CH_2- the shift is owing to two -CH_2- attached to the chain. Hydroxyl group attached -CH_2- carbons appeared at BHET at 61.10 ppm, respectively (Jeya et al., 2017; Jeya et al., 2020) and we were not able to account for the peak appeared at 63.70 ppm. The ^{13}C NMR spectrum of the aminolysed product, BHETA is shown in the supplementary information **(Figure S23)**. The amide carbonyl carbon of BHETA appeared at 167.50 ppm, showing that the amide carbonyl has the structure that confirmed the symmetrical nature of the BHETA single product. Since, BHETA is a symmetrical molecule, there are two aromatic carbons that appeared at 137.10 and 127.60 ppm. The peak at 137.10 ppm corresponds to C-1 and C-4 attached to amide carbonyl, and another peak at127.60 ppm corresponds to C-2, C-3, C-5 and C-6 attached with hydrogen appeared as singlet with high intensity. Two -CH_2- carbons of the aliphatic chain attached to amide -NH- appeared at 42.7 ppm for BHETA. The second hydroxyl group connected to carbon -CH2 appeared at 60.1 ppm of BHETA.

Additionally, functional groups such as hydroxy and amide or ester carbonyl groups present in BHET (**Figure S24)** and BHETA **(Figure S25)** were analyzed through FT-IR. In addition, the molecular weight of BHETA confirmed by the ESI-MS of the aminolysed product **(Figure S26)**. The mass spectrum showed a molecular ion peak at m/z 253.15 that indicated the molecular weight of BHETA.

Conclusions

The present investigation on the depolymerisation of polyethylene terephthalate wastes have been effectively achieved by Lewis acidic ($Zn^{2+}$and Al^{3+}) and heteropolyacids (PWA and PMA) supported kaolin and bentonite catalysts using glycolysis and aminolysis reaction at 150-210°C. The kaolin and bentonite supported catalysts synthesised by the wet-impregnation method at 5wt% of Zn^{2+}, Al^{3+}, PWA and PMA. The crystallinity and structural morphology of the supported catalysts are analysed by X-ray diffraction and SEM. The elemental composition of the catalysts was estimated by using SEM-EDX mapping and XPS analysis. As shown by BET analysis, the surface area of the supported clay catalysts

increased due to occupying of HPA and metal ions in the layered structure of clay. The heteropolyacids loaded catalysts showed better catalytic activity towards glycolytic and aminolytic depolymerisation of PET wastes when compared with Zn^{2+} and Al^{3+} supported catalysts. In comparison to PMA, PWA-supported catalysts showed better performance in depolymerisation of PET wastes. With respect to clay supports, bentonite was found to be the best support for HPA and metal ion loading when compared with kaolin support. The depolymerisation products, bis(2-hydroxyethyl) terephthalate and bis(2-hydroxyethyl) terephthalamide, are formed in the metal ion on top of that kaolin and bentonite. The chemical structure of BHET, BHETA is confirmed with ^{1}H and ^{13}C NMR, FT-IR and MS. Currently, the investigation of glycolysis and aminolysis of waste polyester fabrics using various glycols and aminoalcohols catalyzed by HPA-loaded catalysts is under progress in our laboratory.

Declarations

Acknowledgement

Dr. V. Sivamurugan and Ms. G. Jeya grateful to University Grants Commission (UGC), New Delhi for the financial assistance received in the form of Minor Research Project [MRP-6393/16 (SERO/UGC)]. We thank Ms. Kazuyo Omura at the Institute for Material Research of Tohoku University for XPS measurements. This work was sponsored by JSPS Grant-in-Aid for Scientific Research on Innovative Areas "Discrete Geometric Analysis for Materials Design" (Grant Numbers JP20H04628), JSPS KAKENHI (Grant Numbers JP21H02037), and a cooperative program (Proposal No. 202011-CRKEQ-0001) of CRDAM-IMR, Tohoku University.

Conflict of interest

The authors have declared that there is no conflict of interest.

Samples

Samples of catalysts and depolymerized products are available from the corresponding author.

Authors' Contribution

G.J: Executed laboratory experiments and writing the manuscript, **E.G, A.A.H.T, Y.I:** Characterisation of catalysts, **R.D:** Executed laboratory experiments, **V.S:** Conceptualization, research planning, and manuscript drafting and submission.

References

1. Aher, D.S., Khillare, K.R., Chavan, L.D., Shankarwar, S.G., 2021a. Tungsten-substituted molybdophosphoric acid impregnated with kaolin: effective catalysts for the synthesis of 3,4-dihydropyrimidin-2(1H)-ones via biginelli reaction. RSC Advances. 11, 2783–2792. doi:10.1039/d0ra09811f.

2. Aher, D.S., Khillare, K.R., Shankarwar, S.G., 2021b. Incorporation of Keggin-based H3PW7Mo5O40 into bentonite: synthesis, characterization and catalytic applications. RSC Advances. 11, 11244–11254. doi:10.1039/d1ra01179k.
3. Attique, S., Batool, M., Jalees, M.I., Shehzad, K., Farooq, U., Khan, Z., Ashraf, F., A. T. Shah, A.T., 2018. Highly efficient catalytic degradation of low-density polyethylene Using a novel tungstophosphoric acid/kaolin clay composite catalyst, Turkish Journal Of Chemistry 42. doi:10.3906/kim-1612-21.
4. Al-Sabagh, A.M., Yehia, F.Z., Eshaq, G., Elmetwally, A.E., 2015. Ionic Liquid-Coordinated Ferrous Acetate Complex Immobilized on Bentonite As a Novel Separable Catalyst for PET Glycolysis. Industrial & Engineering Chemistry Research. 54, 12474–12481. doi:10.1021/acs.iecr.5b03857.
5. Bouraie, M.E., Masoud, A.A., 2017. Adsorption of phosphate ions from aqueous solution by modified bentonite with magnesium hydroxide Mg(OH)2. Applied Clay Science. 140, 157–164. doi:10.1016/j.clay.2017.01.021.
6. Chen, L., Nohair, B., Zhao, D., Kaliaguine, S., 2018. Highly Efficient Glycerol Acetalization over Supported Heteropoly Acid Catalysts. ChemCatChem. 10, 1918–1925. doi:10.1002/cctc.201701656.
7. Chen, R., Xin, J., Yan, D., Dong, H., Lu, X., Zhang, S., 2019. Highly Efficient Oxidation of 5-Hydroxymethylfurfural to 2,5-Furandicarboxylic Acid with Heteropoly Acids and Ionic Liquids. ChemSusChem. 12, 2715–2724. doi:10.1002/cssc.201900651.
8. George, N., Kurian, T., 2016. Sodium Carbonate Catalyzed Aminolytic Degradation of PET. Progress in Rubber, Plastics and Recycling Technology. 32, 153–168. doi:10.1177/147776061603200304.
9. Ghosal, K., Sarkar, K., 2019. Poly(ester amide) Derived from Municipal Polyethylene Terephthalate Waste Guided Stem Cell for Osteogenesis. New J. Chem. DOI: 10.1039/C9NJ02940K.
10. Gupta, P., Bhandari, S., 2019. Chemical Depolymerization of PET Bottles via Ammonolysis and Aminolysis. Recycling of Polyethylene Terephthalate Bottles. 109–134. doi:10.1016/b978-0-12-811361-5.00006-7.
11. Jeya, G., Anbarasu, M., Dhanalakshmi, R., Vinitha, V., Sivamurugan, V., 2019. Depolymerization of Poly(ethylene terephthalate) Wastes through Glycolysis using Lewis Acidic Bentonite Catalysts. Asian Journal of Chemistry. 32, 187–191. doi:10.14233/ajchem.2020.22387.
12. Jeya, G., Ilbeygi, H., Radhakrishnan, D., Sivamurugan, V., 2017. Glycolysis of Post-Consumer Poly(ethylene terephthalate) Wastes Using Al, Fe and Zn Exchanged Kaolin Catalysts with Lewis Acidity. Advanced Porous Materials. 5, 128–136. doi:10.1166/apm.2017.1141.
13. Kundu, S.K., Mondal, J., Bhaumik, A., 2013. Tungstic acid functionalized mesoporous SBA-15: A novel heterogeneous catalyst for facile one-pot synthesis of 2-amino-4H-chromenes in aqueous medium. Dalton Transactions. 42, 10515. doi:10.1039/c3dt50947h.
14. Lalhmangaihzuala, S., Laldinpuii, Z., Lalmuanpuia, C., Vanlaldinpuia, K., 2020. Glycolysis of Poly(Ethylene Terephthalate) Using Biomass-Waste Derived Recyclable Heterogeneous Catalyst. Polymers. 13, 37. doi:10.3390/polym13010037.
15. Lamberti, F.M., Román-Ramírez, L.A., Wood, J., 2020. Recycling of Bioplastics: Routes and Benefits. Journal of Polymers and the Environment. 28, 2551–2571. doi:10.1007/s10924-020-01795-8.

16. Langer, E., Bortel, K., Waskiewicz, S., Lenartowicz-Klik, M., 2020. Methods of PET Recycling. Plasticizers Derived from Post-Consumer PET. 127–171. doi:10.1016/b978-0-323-46200-6.00005-2.
17. Maurya, A., Bhattacharya, A., Khare, S.K., 2020. Enzymatic Remediation of Polyethylene Terephthalate (PET)–Based Polymers for Effective Management of Plastic Wastes: An Overview. Frontiers in Bioengineering and Biotechnology 8. doi:10.3389/fbioe.2020.602325.
18. Morgan, A.B., Harris, J.D., 2004. Exfoliated polystyrene-clay nanocomposites synthesized by solvent blending with sonication. Polymer. 45, 8695–8703. doi:10.1016/j.polymer.2004.10.067.
19. Munir, M., Ahmad, M., Saeed, M., Waseem, A., Rehan, M., Nizami, A.-S., Zafar, M., Arshad, M., Sultana, S., 2019. Sustainable production of bioenergy from novel non-edible seed oil (Prunus cerasoides) using bimetallic impregnated montmorillonite clay catalyst. Renewable and Sustainable Energy Reviews. 109, 321–332. doi:10.1016/j.rser.2019.04.029.
20. Nagasundaram, N., Kokila, M., Sivaguru, P., Santhosh, R., Lalitha, A., 2020. SO3H@carbon powder derived from waste orange peel: An efficient, nano-sized greener catalyst for the synthesis of dihydropyrano[2,3-c]pyrazole derivatives. Advanced Powder Technology. 31, 1516–1528. doi:10.1016/j.apt.2020.01.012.
21. Naswir, M., Arita, S., Marsi, Salni, 2013. Characterization of Bentonite by XRD and SEM-EDS and Use to Increase PH and Color Removal, Fe and Organic Substances in Peat Water. Journal of Clean Energy Technologies. 313–317. doi:10.7763/jocet.2013.v1.71.
22. Russell, J.D., Fraser, A.R., 1994. Infrared methods. Clay Mineralogy: Spectroscopic and Chemical Determinative Methods. 11–67. doi:10.1007/978-94-011-0727-3_2.
23. Sarkar, K., Meka, S.R.K., Bagchi, A., Krishna, N.S., Ramachandra, S.G., Madras, G., Chatterjee, K., 2014. Polyester derived from recycled poly(ethylene terephthalate) waste for regenerative medicine. RSC Adv. 4, 58805–58815. doi:10.1039/c4ra09560j.
24. Shuangjun, C., Weihe, S., Haidong, C., Hao, Z., Zhenwei, Z., Chaonan, F., 2020. Glycolysis of poly(ethylene terephthalate) waste catalyzed by mixed Lewis acidic ionic liquids. Journal of Thermal Analysis and Calorimetry. 143, 3489–3497. doi:10.1007/s10973-020-10331-8.
25. Shukla, S.R., Palekar, V., Pingale, N., 2008. Zeolite catalyzed glycolysis of poly(ethylene terephthalate) bottle waste. Journal of Applied Polymer Science. 110, 501–506. doi:10.1002/app.28656.
26. Singh, N., Hui, D., Singh, R., Ahuja, I., Feo, L., Fraternali, F., 2016. Recycling of plastic solid waste: A state of art review and future applications. Composites Part B: Engineering. 115, 409–422.
27. Singh, N., Hui, D., Singh, R., Ahuja, I., Feo, L., Fraternali, F., 2017. Recycling of plastic solid waste: A state of art review and future applications. Composites Part B: Engineering. 115, 409–422. doi:10.1016/j.compositesb.2016.09.013.
28. Sinha, V., Patel, M.R., Patel, J.V., 2010. Pet Waste Management by Chemical Recycling: A Review. Journal of Polymers and the Environment. 18, 8–25. doi:10.1007/s10924-008-0106-7.
29. Siregar, S.H., Wijaya, K., Kunarti, E.S., Syoufian, A., Suyanta, 2017. Preparation and Characterization of Montmorillonite-Cetyl Trimethylammonium Bromide. Asian Journal of Chemistry. 30, 25–28. doi:10.14233/ajchem.2018.20782.

30. Wang, Q., Yao, X., Geng, Y., Zhou, Q., Lu, X., Zhang, S., 2015. Deep eutectic solvents as highly active catalysts for the fast and mild glycolysis of poly(ethylene terephthalate)(PET). Green Chemistry. 17, 2473–2479. doi:10.1039/c4gc02401j.
31. Winiarski, J., Tylus, W., Winiarska, K., Szczygieł, I., Szczygieł, B., 2018. XPS and FT-IR Characterization of Selected Synthetic Corrosion Products of Zinc Expected in Neutral Environment Containing Chloride Ions. Journal of Spectroscopy. 1–14. doi:10.1155/2018/2079278.

Figures

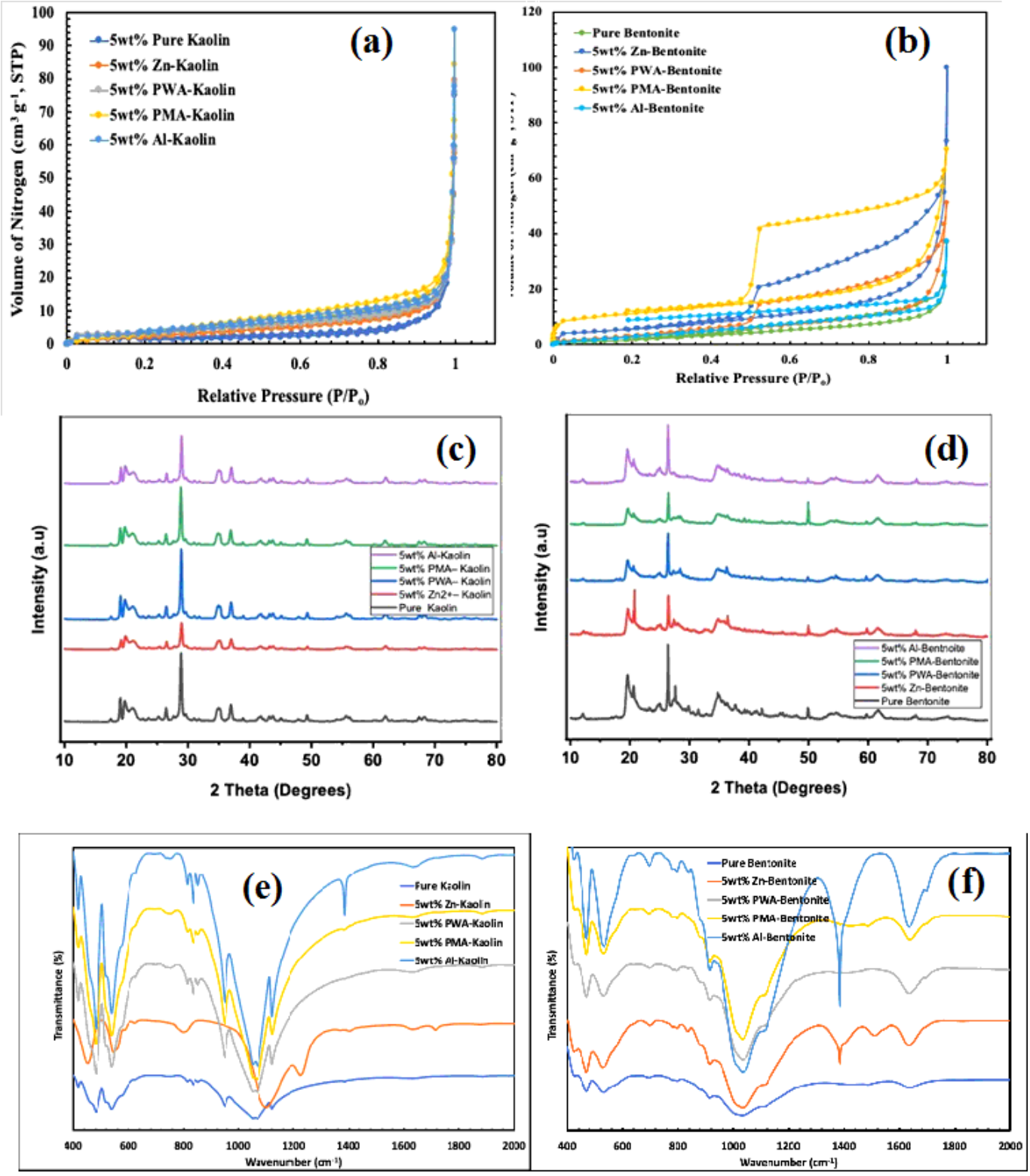

Figure 1

(a) and (b) BET isotherm Al3+, Zn2+, PWA and PMA supported Kaolin and Bentonite Catalysts; (c) and (d) XRD patterns; (e) and (f) FT-IR spectra of Al3+, Zn2+, PWA and PMA supported Kaolin and Bentonite Catalysts

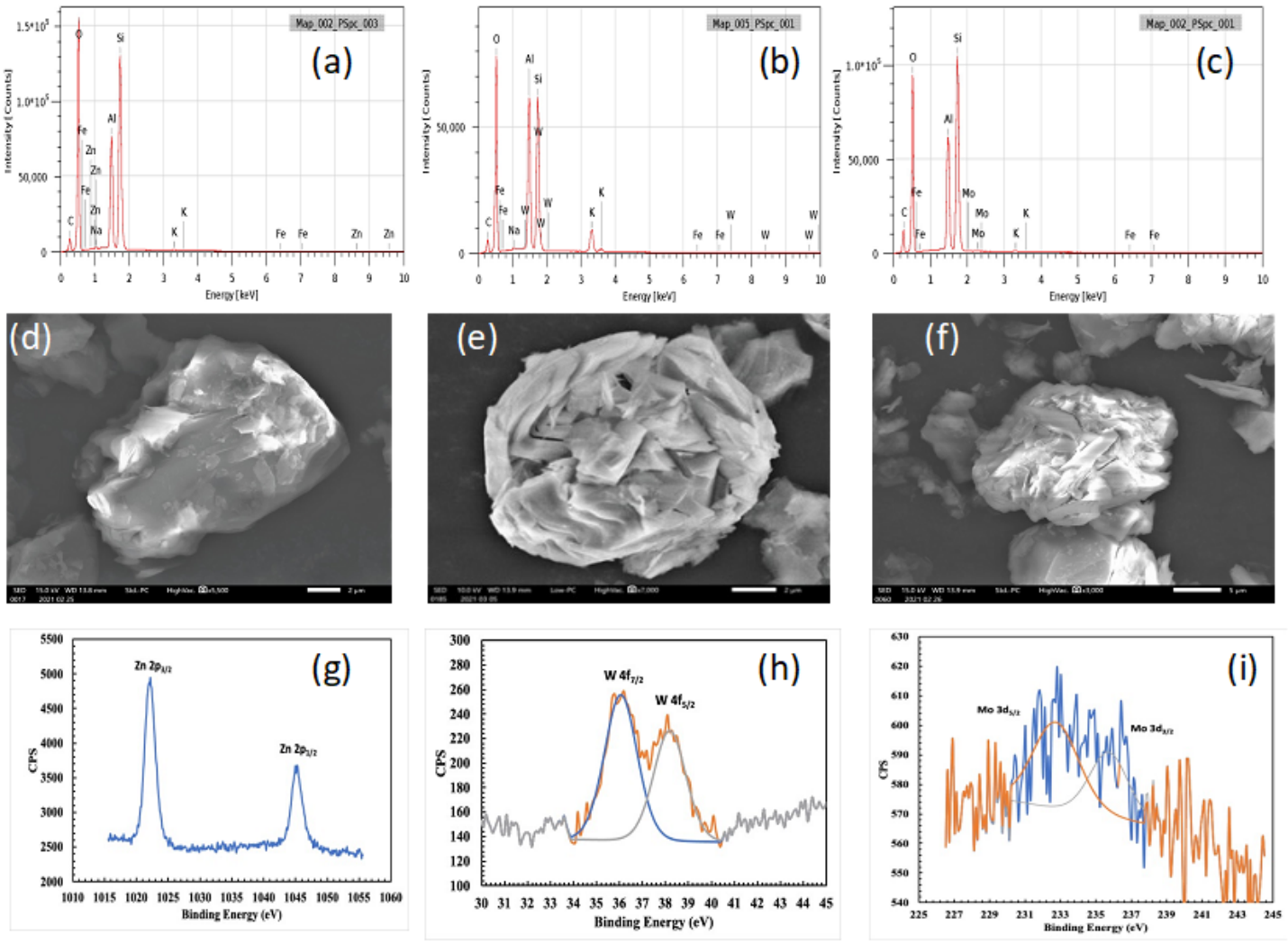

Figure 2

(a), (b) and (c) EDAX spectrum; (d), (e) and (f) SEM images; (g), (h) and (i) XPS spectra of Zn2+, PWA and PMA supported Kaolin Catalysts

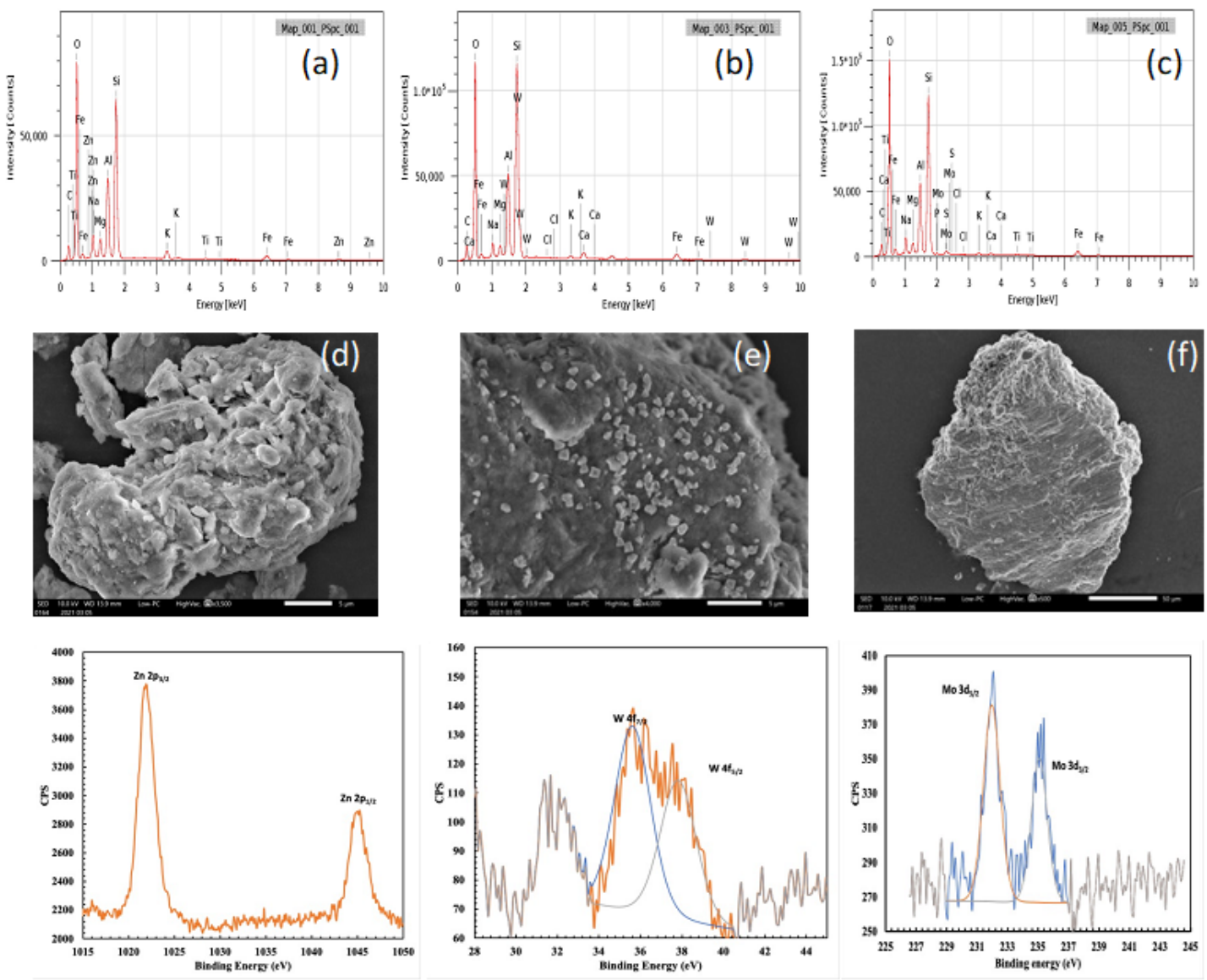

Figure 3

(a), (b) and (c) EDAX spectrum; (d), (e) and (f) SEM images; (g), (h) and (i) XPS spectra of Zn2+, PWA and PMA supported Bentonite Catalysts

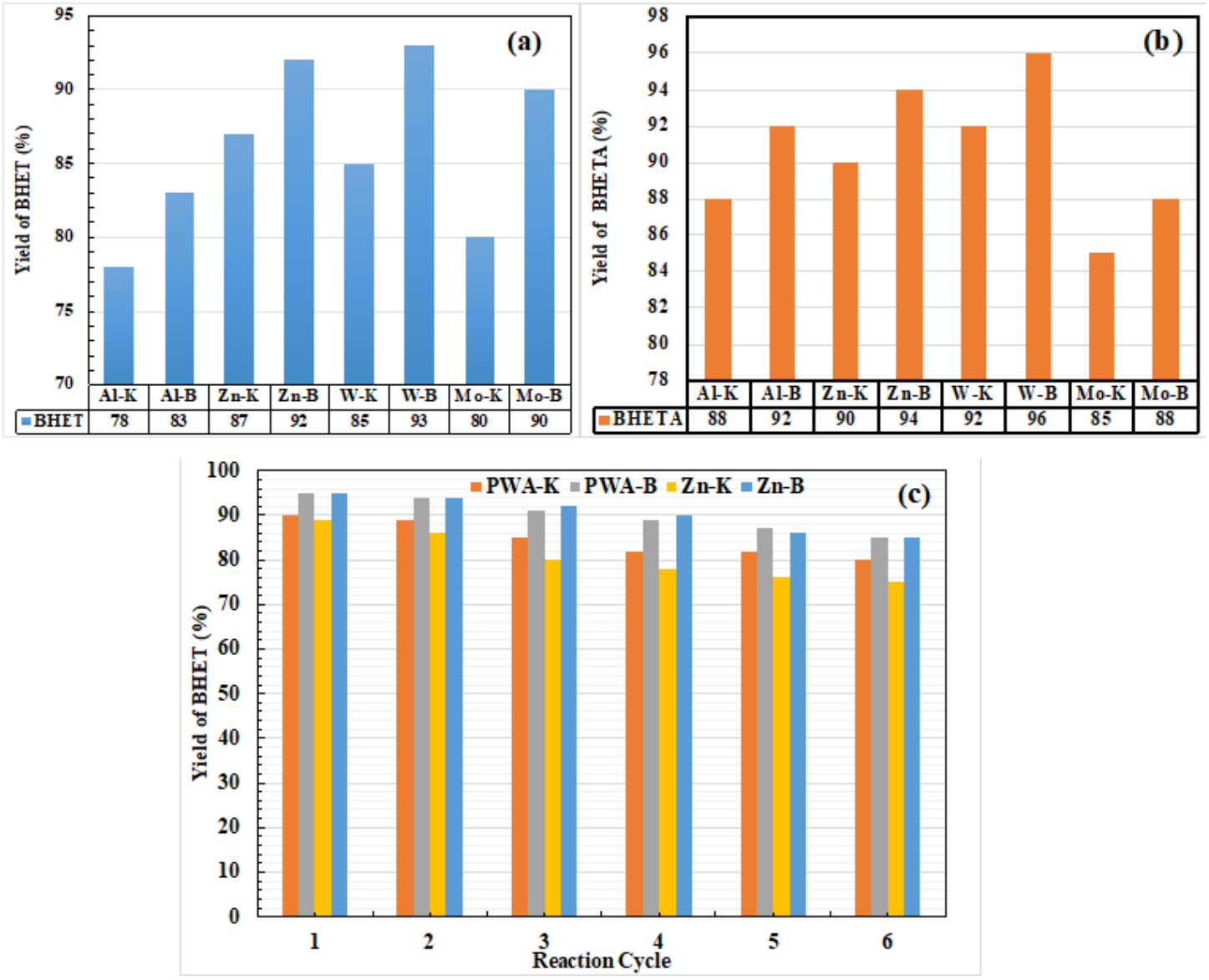

Figure 4

(a) Glycolysis of PET wastes; (b) Aminolysis of PET wastes using Al3+, Zn2+, PWA and PMA on Kaolin (K) and Bentonite (B); (c) Catalysts recycling studies using PWA and Zn2+ loaded Kaolin (K) and Bentonite (B)

Supplementary Files

This is a list of supplementary files associated with this preprint. Click to download.

- Supplementaryinformation01102021.docx
- Onlinefloatimage1.png